applied sciences

MDPI

Article

Implementation and Evaluation of a Uterine Manipulation System Incorporated with an Existing Tiltable-Tip Uterine Manipulator for Gynecological Laparoscopy

Songphon Namkhun [1], Kovit Khampitak [2], Apiwat Boonkong [3] and Daranee Hormdee [1,*]

[1] Department of Computer Engineering, Faculty of Engineering, Khon Kaen University, Khon Kaen 40002, Thailand; songphon.n@kkumail.com
[2] Department of Obstetrics and Gynecology, Faculty of Medicine, Khon Kaen University, Khon Kaen 40002, Thailand; kovit@kku.ac.th
[3] Department of Computer Engineering, Faculty of Engineering, Nakhon Phanom University, Nakhon Phanom 48000, Thailand; apiwat.boon@npu.ac.th
* Correspondence: darhor@kku.ac.th

Abstract: In gynecologic surgery, a uterine manipulator is one of the instruments used to perform the laparoscopy. Throughout the past decade, a number of robotic technology applications used for uterine manipulation during surgery have been designed with the aim of increasing the efficiency, improving the precision, and reducing the workload of medical assistants. Although the RCM (Remote Center of Motion) mechanism is one of the key features in a Minimally Invasive Surgical (MIS) robot, the preliminary result in this study, in which the RCM mechanism was applied in a uterine manipulation robot, proved that this may cause unpleasant sensations such as irritation or harm to the nearby area during such manipulation. Therefore, a design of a non-RCM 2-DoF (Degree of Freedom) Robotic Uterine Manipulation System, in cooperation with an existing, reusable and tiltable-tip uterine manipulator, for laparoscopic gynecologic surgery has been proposed and evaluated via a mathematical model along with numerical analysis, a 3D uterus model, and a 1:1 uterus manikin model in order to demonstrate the use of the essential functions. According to the experimental results, the maximum load of 500 g has been handled well by the prototype, with the movement ranges of ±150° in the roll panel and ±90° in the pitch panel (0∼90° for anteversion and 0∼−90° for retroversion, if needed, which can be achieved by rotating the instrument to the other side). Furthermore, to verify this new design prior to its use on patients, and also in consideration of the ethics of human experimentation, through extensive testing on five donated soft-tissue cadavers, the proposed robot received positive feedback from all five surgeons performing the experiments and could offer effective uterine manipulation at the angular velocity of 4 °/s (0.67 RPM) with steady delineation of the vaginal fornices to create necessary motions in the pitch and roll panels of 30∼80° and ±15°, respectively, providing efficient visualization of the uterus. These features make this robot a valuable addition to the surgical instruments available to gynecologic surgeons.

Keywords: uterine manipulation; gynecological laparoscopy; surgical robot; tiltable-tip uterine manipulator

Citation: Namkhun, S.; Khampitak, K.; Boonkong, A.; Hormdee, D. Implementation and Evaluation of a Uterine Manipulation System Incorporated with an Existing Tiltable-Tip Uterine Manipulator for Gynecological Laparoscopy. *Appl. Sci.* **2024**, *14*, 3851. https://doi.org/10.3390/app14093851

Academic Editor: Fausto Famà

Received: 16 March 2024
Revised: 27 April 2024
Accepted: 29 April 2024
Published: 30 April 2024

1. Introduction

Minimally Invasive Surgery (MIS) has played an important role in healthcare for over two decades, promoting patient safety by significantly reducing the level of invasion, as the surgical end effectors are inserted through small incision ports. MIS can be used to treat a number of gynecologic conditions, in which the position of the uterus is essential [1]. Figure 1 illustrates how the operating theater for Laparoscopic Gynecologic Surgery is usually set up. The common setup comprises Surgeon (**S**), Patient (**P**), Nurse

(**N**), Anesthetist (**A**) and Monitor (**M**) showing the image transferred from the laparoscope. Figure 1a,c show the setups for conventional laparoscopic surgery, in which **L**, representing the assistant holding and controlling the Laparoscope, is necessary. Figure 1b,d are the setups of Robot-Assisted Surgery (RAS). This replaces **L**, with the robot depicted in the semi-sphere equipment here used to manipulate the scope. Unlike traditional open surgery, in laparoscopic gynecological surgery, the uterus is not controlled directly through small incisions. **U** in Figure 1a,b represents an assistant in charge of the uterine manipulation, whereas **R** represents the designed uterine manipulator robot, which can easily be applied to either conventional laparoscopic surgery or RAS, as shown in Figure 1c,d, respectively.

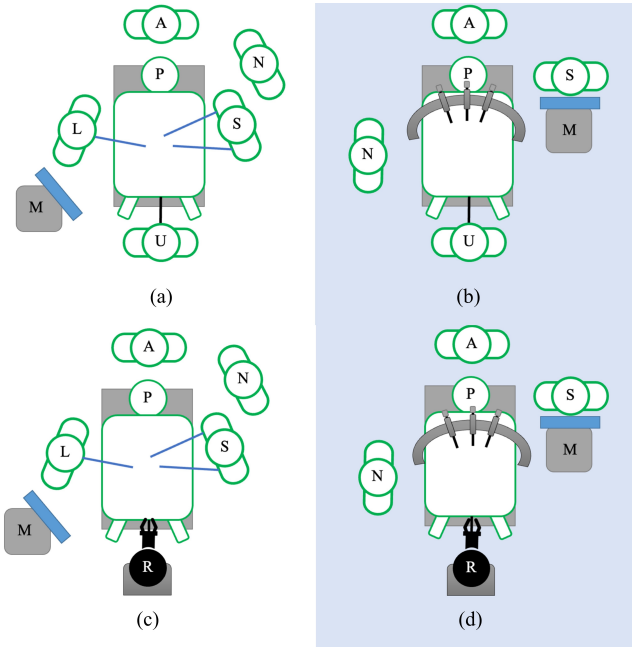

Figure 1. Diagrams of operating theater setups for conventional laparoscopic surgery in (**a**,**c**) and for RAS in (**b**,**d**) where in (**a**,**b**) is with an assistance holding the uterine manipulator and in (**c**,**d**) with a uterine manipulator robot.

To date, two approaches have been used to manipulate the uterus: abdominal control [2] and vaginal control, in compliance with the MIS scheme. In this approach, a uterine holder/manipulator, inserted through the patient's vulva, has become widely used, particularly during hysterectomies, as it offers several benefits to the laparoscopic surgeon due to the lateral mobilization of the uterus. In the last few decades, several new uterine manipulators have been developed. It has been stated [3] that the use of a uterine manipulator is one of the success factors for improving total laparoscopic hysterectomy (TLH). Uterine manipulation has evolved over the years. Initially, both the manipulation and holding of the uterine manipulator were performed manually; then, the uterine manipulation was performed by a human but an instrument held the manipulator itself [4–7]; finally, a robot performed the manipulation of the uterus and held the uterine manipulator. Examples of uterine manipulation robots can be seen in both the market and previous publications [8–16]. All of these robots were specifically built to carry out the entire process with a great deal of complexity.

This study not only aims to implement a fatigue-free robotic uterine manipulation system which should be compatible with an existing and reusable uterine manipulator, but also seeks to achieve simplicity along with efficiency of implementation. Incorporating a familiar/existing uterine manipulator, the proposed system can be directly manipulated by the main surgeon to take up the task of uterus manipulation during laparoscopic gynecologic surgery.

2. Literature Review

With the body of a mature size, the average dimensions of a uterus [17] in a reproductive-age female are 8 cm long, 5 cm wide, and 4 cm thick, with the varied weight from a few hundred grams up to over five kilograms for extreme cases. Looking at uterus movement in three-dimensional space, the position of an object is commonly represented in space using three axes: the lateral (X)-axis, longitudinal (Y)-axis, and vertical (Z)-axis. And the technical terms for the rotation of each axis are **Roll** for the rotation about the Y-axis (in red); **Pitch** for the rotation about the X-axis (in purple) and **Yaw** for the rotation about the Z-axis (in blue), shown in Figure 2. The term Degrees of Freedom or DoF is widely used to define the number of independent motions through which a rigid object can move through 3D space. It refers to the ability of the robot to move **backward–forward** (Y-axis), **left–right** (X-axis), **up–down** (Z-axis), **Roll**, **Pitch** and **Yaw**. An object requires six Degrees of Freedom, three linear movements, and three rotationally movements to be completely free to change position.

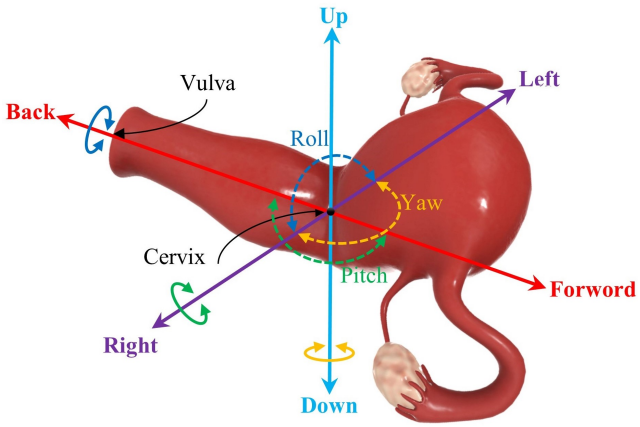

Figure 2. Three dimensions of movement.

There are a number of uterine manipulators available in the market [18]. The main criteria for choosing a uterine manipulator are fixed-tip [19] vs. tiltable-tip (Distal Pitch) [20] vs. flexible-tip [21,22] and disposable (Clearview Manipulator) vs. reposable (Rumi Manipulator) vs. reusable (Clermont Ferrand, Keckstein, Valtchev, and Tintara) [23].

In the past decade, several uterine manipulation robots have been implemented as listed in Table 1, with the choices of using RCM (Remote Center of Motion) mechanism [24] vs. Non-RCM as the motion mechanism; whether incorporating a tiltable-tip or fixed-tip manipulator; whether the manipulator is reusable (as, for economic reasons, reusable surgical instruments are worthy of consideration); and lastly whether the chosen manipulator is available in the market, and hence there is no need to acquaint the surgeon with the new design/implementation of the instrument. The different uterus movements, controlled by a uterine manipulator, have been categorized as shown in Figure 3.

Table 1. Uterine manipulator robots.

Name	Uterus Movement	Mechanism	Tiltable-Tip	Reusable	Existing
ViKY UP [8,9]	Figure 3a	RCM@Vulva	x	x	/
Premachandra [12]	Figure 3b	RCM@Cervix	x	/	/
Wu et al. I [13]	Figure 3b	RCM@Cervix	x	/	/
Yip et al. [10,11]	Figure 3c	RCM@Cervix	x	/	/
Wu et al. II [14]	Figure 3d	RCM@Cervix	/	x	x
Tsai et al. [15]	Figure 3e	non-RCM	/	x	x
Nguyen et al. [16]	Figure 3e	non-RCM	/	x	x
Mustaza [21]	Figure 3f	non-RCM	/	x	x
Lee [22]	Figure 3f	non-RCM	/	x	x

The benefit of the RCM mechanism [25], one of the key features in MIS robots, is to maintain a stable entry point into the body by lessening the invasion level, avoiding damage on the surrounding tissue, while allowing the surgeon to manipulate the instruments' pivot around their incision ports with precision and dexterity.

Recently, the applications of RCM have expanded from the main robotic surgical systems to robotic uterine manipulators [8–14]. ViKY products provide obvious examples of how the RCM mechanism has evolved from application on a main laparoscopic robot, ViKY Endoscope Positioner (ViKY EN) [9], to a uterine manipulator robot, the ViKY Uterus Positioner (ViKY UP) [8]. Both RCM points of ViKY Positioners are located at the skin incision ports, which can be found at the vulva for ViKY UP (Figure 3a). However, according to the anatomy of the pelvic [26], it is more sensible to lock the RCM point at the cervix, as can be seen in all RCMs in later works, as listed in Figure 3.

Meanwhile, there are uterine manipulator robots that do not use the RCM mechanism due to the use of instruments with a tiltable-tip [15,16] (Figure 3e) and a flexible-tip robot [21,22] (Figure 3f).

The device with a tip that allows insertion/extraction is used to adjust the length of the device according to the size of the cervix. However, for devices with adjustable tips, the size of the tip can be changed to match the size of the cervix. Since surgeons are the ones who install the device into the cervix themselves, the insertion/extraction movement is not utilized.

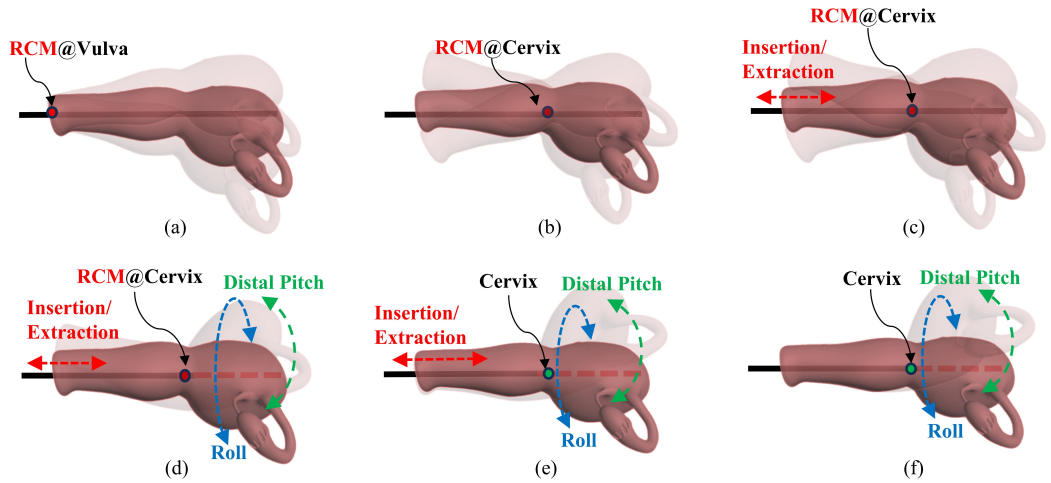

Figure 3. Movement of uterus: with (**a**) RCM@vulva, (**b**) RCM@cervix (**c**) RCM@cervix with insertion/extraction motion, (**d**) RCM@cervix with insertion/extraction, **Roll** and distal **Pitch** motions, (**e**) no RCM but with insertion/extraction, **Roll** and distal **Pitch** motions, (**f**) no RCM but with **Roll** and distal **Pitch** motions.

The choice of the uterine manipulator depends on the indication. Furthermore, some previous studies [18,27] remarked that the choice of uterine manipulator did not affect the surgical results except for the duration of the operation, and hence it has never been concluded which uterine manipulator is optimal. Having said that, though, with the help of tenaculum forceps, which are used to hold and stabilize the cervix, it is rather difficult to protect the vulva along with the cervix when using a fixed-tip uterine manipulator. Concerning a fixed-tip uterine manipulator, incorporating the RCM mechanism could fulfill the control range of uterine movements. However, unlike in MIS robots, in which the RCM point is fixed to a surgical incision to minimize the incision, in order to protect the cervix of the uterus, the uterine manipulator is inserted through the vulva with the RCM point fixed mostly to the cervix. As can be seen in Figure 4, the movement of the vulva would show a motion which is in reverse to the way the uterus is maneuvered, as shown in Figure 4a. The average vaginal length [17] from vulva to a cervix is 9.6 cm, which means that the transition distance of the vulva could vary corresponding to the angle at which the

manipulator moves. Per Equation (1), to find the Base (**B**) as in an isosceles triangle, in this case, illustrated in Figure 4a, where Side (**S**) is the vaginal length of 9.6 cm, **B** represents how much the vulva would move from the origin point which, according to the angle $\boldsymbol{\varphi}$ of (15∼90°), is 2.51–13.58 cm, as shown in Table 2. And this can be a bigger transition distance for a longer cervix, leading to unpleasant sensations, irritation, or harm to the vulva.

$$Base = 2 \times Side \times \sin(\frac{\boldsymbol{\varphi}}{2}) \quad (1)$$

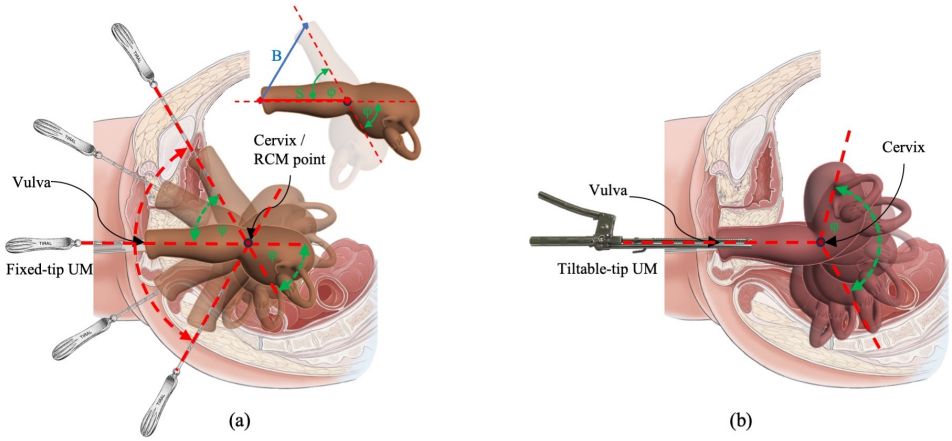

Figure 4. Movement of uterus and vulva; with (**a**) a fixed-tip uterine manipulator and (**b**) a tiltable-tip uterine manipulator.

Table 2. Bases corresponding to different angles $\boldsymbol{\varphi}$.

Angle $\boldsymbol{\varphi}$ (°)	**15°**	**30°**	**45°**	**60°**	**75°**	**90°**
Base (cm)	2.51	4.97	7.35	9.60	11.69	13.58

Figure 4b illustrates the possible movement of the uterus along with the cervix and vulva when applying a tiltable-tip uterine manipulator in a straightforward manner, without using the RCM mechanism. The joint between the tip and the body of the uterine manipulator would sit at the cervix so the movement of the tip would control the uterus alone, while the rest of the body would remain in place, stabilizing the vulva.

After reviewing the previous related works on robotic uterine manipulation systems, regarding an existing uterine manipulator, we have determined that acquainting the surgeon with the new design/implementation of the instrument would not be necessary. And, for economic reasons, reusable surgical instruments are worthy of consideration. Lastly, choosing a tiltable-tip instrument in this study, incorporated with a well-designed actuator mechanism, meant that there was no need to use the RCM, resulting in a much simpler design to fulfill the requirement of uterine manipulation.

As a result, the contribution of this paper is to implement a robotic uterine manipulation system in potential collaboration with an existing, reusable, and tiltable-tip uterine manipulator. The rest of the paper describes the implementation and comprehensive evaluations of this simplified system design. Furthermore, given that any new technology should be extensively and thoroughly tested via various simulations and experiments prior to implementation in gynecological surgery and testing on patients [28], a number of research models, including a mathematical model with numerical analysis, a 3D uterus model, a manikin model and soft-tissue cadaver cases, have also been evaluated here.

3. Implementation and Design

The process of implementing the proposed uterine manipulator robot, shown in Figure 5, begins with the chosen instrument with tiltable-tip, which is reusable and available in the market. Later, the kinematic design of the proposed uterine manipulation robot

is presented, followed by its simulation results on a mathematical model and 3D models. In order to obtain force requirements for the relevant equipment, force testing is undertaken. Then, using all the available equipment, once the prototype has been designed and implemented, a number of tests, described and demonstrated later in the paper, including testing with a uterus manikin model and finally testing on soft-tissue cadavers, are determined to ensure the operational validation of the proposed system.

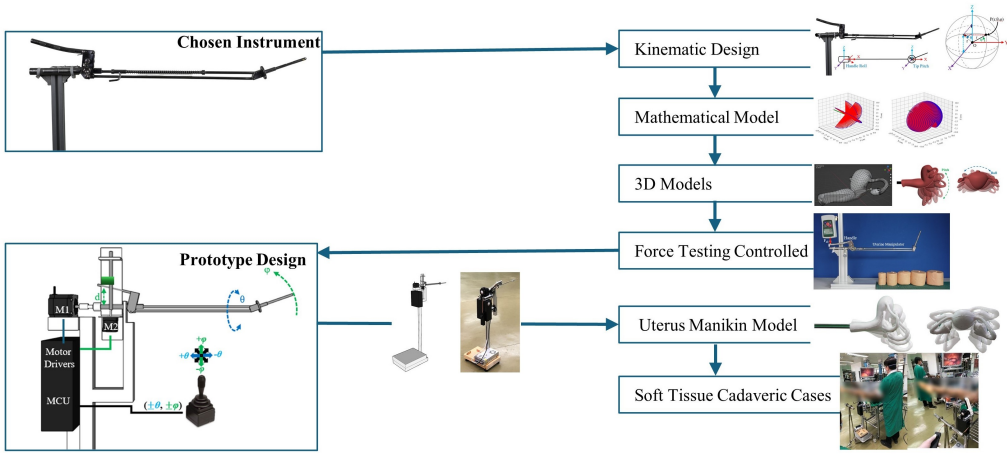

Figure 5. Diagram of robot prototype implementation and preoperative performance evaluation in soft-tissue cadavers.

3.1. Chosen Instrument

As per the previous section, with the aim to of simplifying the robotic system to ensure its compatibility with an existing instrument, the uterine manipulator used here has been selected from the available reusable tiltable-tip uterine contraction instruments. Similarly to other tiltable-tip uterine manipulators, the chosen uterine manipulator, which is almost identical to the Tintara uterine manipulator [20] shown in Figure 6, consists of three parts; a handle, a body, and a tiltable tip. Its body comprises two stainless-steel rods and a spring hook retaining its contact with the tenaculum. At the joint connecting the body and the tiltable-tip, a plate is connected to the changeable pivot head with a screw. The head has a diameter of 5 mm with three standard lengths of 6, 8, and 10 cm. This instrument allows anteversion of the uterus up to 90° and lateral motion of about 150° bilaterally.

Unlike other uterine manipulator robots, which may require 3 DoFs [8,10,14], 5 DoFs [12] or up to 7 DoFs [13], the 2 DoFs of the chosen uterine manipulator could provide a considerably sufficient coverage of uterine movements, delineate the vaginal fornices nicely and allow the uterus to flex on itself.

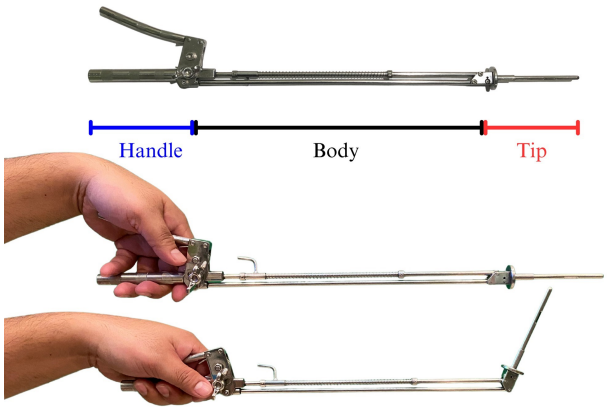

Figure 6. The chosen tiltable-tip uterine manipulator.

Though the movement control range of the chosen instrument could achieve nearly the full coverage of an entire sphere, it is not that straightforward for the **Roll**, **Yaw** and **Pitch** motions. As shown in Figure 7, there are two joints in the chosen instrument at the handle and the tip at which the handle can only roll while the tip can only tilt; these will be referred to as (handle) **Roll** and (tip) **Pitch**, respectively, from now on. Though the instrument can only maneuver ±150° (not the full 360° in the **Roll** panel due to the handle of the instrument, which is the most unwieldy part) in roll motion, and only (0∼90°) in tilt or pitch motion due to its structure, with the combination of these roll and tilt maneuvers, **Pitch** and **Yaw** panels can be achieved. In total, generally speaking, the chosen instrument can move ±150° in the **Roll** panel and ±90° in both **Pitch** and **Yaw** panels.

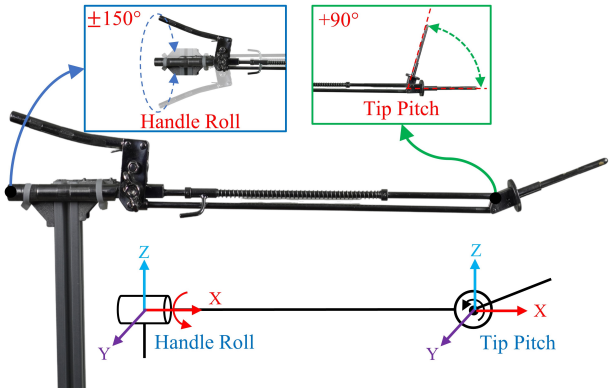

Figure 7. Configuration of the 2 DoFs of the chosen instrument.

Figure 8 illustrates the movements in the **Roll**, **Yaw**, and **Pitch** panels of the chosen manipulator, with the body pointing towards the front, showing the best views of the tip: the front views, as shown in Figure 8a,c, and the side view, as shown in Figure 8b,d, where the vertical stick is the pole, holding the instrument. Figure 8a shows the **Roll** motion of ±150° with the **Pitch** angle fixed to 90°. Though the distal **Yaw** motion cannot be manipulated directly via the manipulator, any designated position in the **Yaw** panel could be achieved as shown in Figure 8c by controlling the **Roll** motion followed by the **Pitch** motion. Lastly, both Figure 8b,d depict the movement in the **Pitch** panel. Although the **Pitch** motion can be directly achieved by varying the **Pitch** angle, the movement in Figure 8b is limited to only (0∼90°) in the **Pitch** panel, as the instrument cannot roll down to 180° due to the bulky handle, while Figure 8d shows all ±90° in the **Pitch** panel when the instruments rolls to other available angles. Here, the first half of the **Pitch** angles (0∼90°) can be obtained with a **Roll** angle (30°) and the last half of the **Pitch** angles (0∼−90°) can be obtained with the flipped **Roll** angle (−150°).

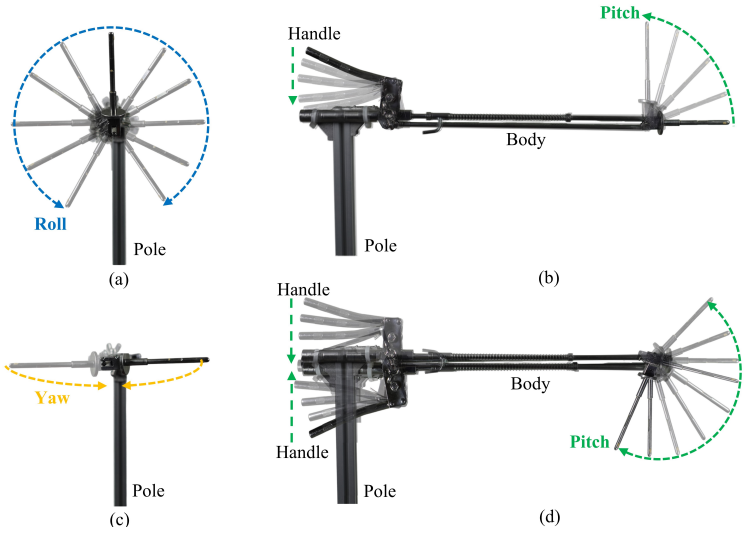

Figure 8. Coverage of uterine manipulator movement; (**a**) is the front view showing the ±150° in the **Roll** panel with the **Pitch** angle fixed to 90°, (**b**) is the side view showing the (0∼90°) in the **Pitch** panel, (**c**) is the front view showing how the distal **Yaw** motion could be achieved and (**d**) is the side view showing all ±90° in the **Pitch** panel.

3.2. Kinematic Design

This section explains the kinematic design of the proposed uterine manipulation robot. Figure 9a shows the spherical coordinates with the origin (**O**) or pole fixed at the cervix. According to **Roll** and **Pitch** motions on the selected uterine manipulator, the movement would occur in spherical coordinates (**r**, ***θ***, ***φ***), where the radial distance (**r**) is the tip length, the azimuthal angle (***θ***) made by the **Roll** motion and polar angle (***φ***) made by the **Pitch** motion of a point (**P**) with respect to a unit sphere with a fixed point (**O**), as shown in Figure 9b. The movements at the handle that cause **Roll** and **Pitch** motions have been illustrated in blue and green, respectively.

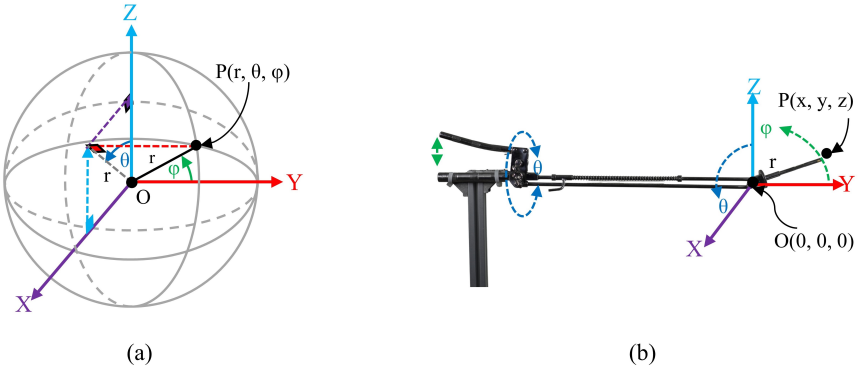

Figure 9. Coordinate system design; (**a**) spherical coordinates and (**b**) mapping on the uterine manipulator.

As can be seen in the Spherical coordinates, with known **r** for radius, ***θ*** for **Roll** motion and ***φ*** for **Pitch** motion, it is sufficient for a coordinate to be located anywhere on the spherical object area, hence there is no need for a direct Yaw motion transition. However, with regard to the control interfacing, the Cartesian coordinate system, in which the coordinates are perpendicular to one another with the same unit length on all **XYZ**-axes, is essential. Therefore, conversion between Spherical coordinates and Cartesian coordinates is needed. Equations (2)–(4) are the calculation of (**r**, ***θ***, ***φ***) coordinates from the Cartesian coordinates while Equations (5)–(7) are the calculation of (x, y, z) coordinates from the Spherical coordinates. Next, the simulation results from this kinematic design have been evaluated by a mathematical model and 3D models.

$$\mathbf{r}^2 = \mathbf{x}^2 + \mathbf{y}^2 + \mathbf{z}^2 \quad (2)$$

$$\boldsymbol{\varphi} = \cos^{-1}\left(\frac{\mathbf{x}}{\mathbf{r}}\right) \tag{3}$$

$$\boldsymbol{\theta} = \tan^{-1}\left(\frac{\mathbf{y}}{\mathbf{z}}\right) \tag{4}$$

$$\mathbf{x} = \mathbf{r} \times \cos(\boldsymbol{\theta}) \tag{5}$$

$$\mathbf{y} = \mathbf{r} \times \sin(\boldsymbol{\varphi}) \sin(\boldsymbol{\theta}) \tag{6}$$

$$\mathbf{z} = \mathbf{r} \times \sin(\boldsymbol{\varphi}) \cos(\boldsymbol{\theta}) \tag{7}$$

3.3. Mathematical Model

The performance of the kinematic design has been evaluated by mathematical modeling via a Matplotlib [29] module, using the Cartesian and Spherical coordinate conversion equations to represent the current coordinates. Figure 10 illustrates the mathematical modeling results when varying either the azimuthal angle ($\boldsymbol{\theta}$) or the polar angle ($\boldsymbol{\varphi}$), or both. Figure 10a–c show how **Yaw** motion can be achieved in this system. Although it cannot be achieved straightforwardly, but necessitates fixing $\boldsymbol{\theta}$ to 90° and varying $\boldsymbol{\varphi}$ from 0∼90°, the first half of the movement in the **Yaw** panel can be obtained (Figure 10a). Then, moving $\boldsymbol{\varphi}$ back to 0° and then fixing $\boldsymbol{\theta}$ to −90° and varying $\boldsymbol{\varphi}$ from 0∼90°, the second half of the panel can be fulfilled (Figure 10b). Furthermore, to illustrate the coordinate trajectories in the **Roll** panel, by varying the $\boldsymbol{\theta}$ in the **Roll** panel between ±150°, Figure 10d shows how the $\boldsymbol{\varphi}$ is fixed to 30° and 60°. Additionally, Figure 10e shows the coordinate trajectories in the **Pitch** panel (varying the $\boldsymbol{\varphi}$ in the **Pitch** panel from 0∼90°) when $\boldsymbol{\theta}$ is fixed to five positions, including 0°, ±45°, and ±135°. Lastly, Figure 10f depicts the whole coverage (nearly the entire sphere) which is caused by varying $\boldsymbol{\theta}$ between ±150° (hence not a full sphere) and $\boldsymbol{\varphi}$ varied from 0∼90°.

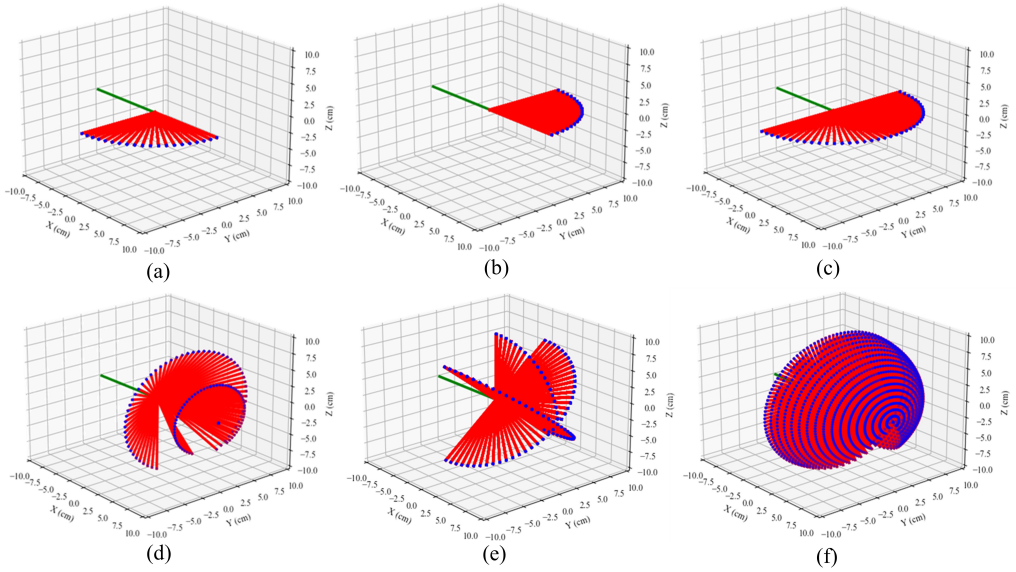

Figure 10. The entire coordinate trajectory of the chosen manipulator; (**a**) the first half motion in the **Yaw** panel, (**b**) the second half motion in the **Yaw** panel, (**c**) the whole motion in the **Yaw** panel, (**d**) example motions in the **Roll** panel, (**e**) example motions in the **Pitch** panel, and (**f**) the entire motion in all panels.

3.4. Three-Dimensional Uterus Model

After exploring the coverage this uterine manipulator could offer, a 3D uterus model, as shown in Figure 11, was built with all the bones/joints made using Blender software [30]. Figure 12 illustrates the finished 3D uterus model with the labels of relevant terms. In order to visualize the movement patterns and to ensure that the robot control equation works properly, the model was then imported for testing in Unity software.

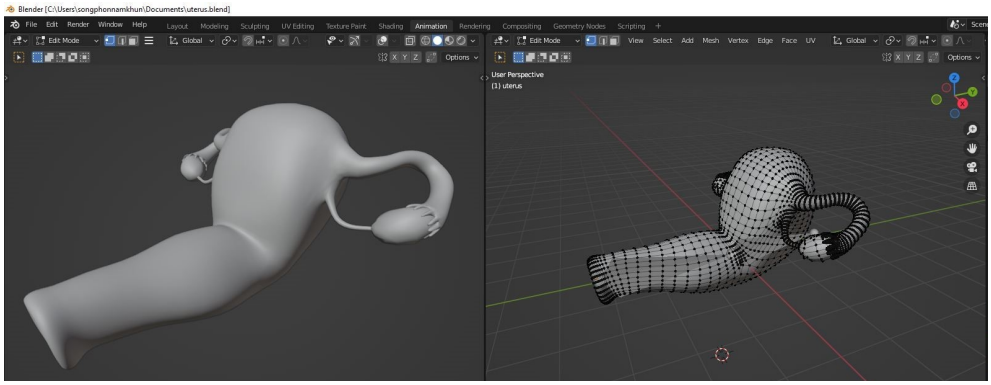

Figure 11. Building a 3D uterus model in Blender.

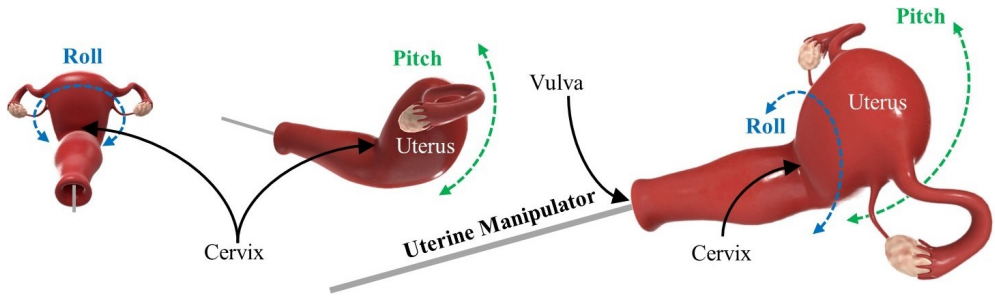

Figure 12. A 3D uterus model.

Figure 13 shows the movement of a uterine manipulator along **Roll** and **Pitch** panels.

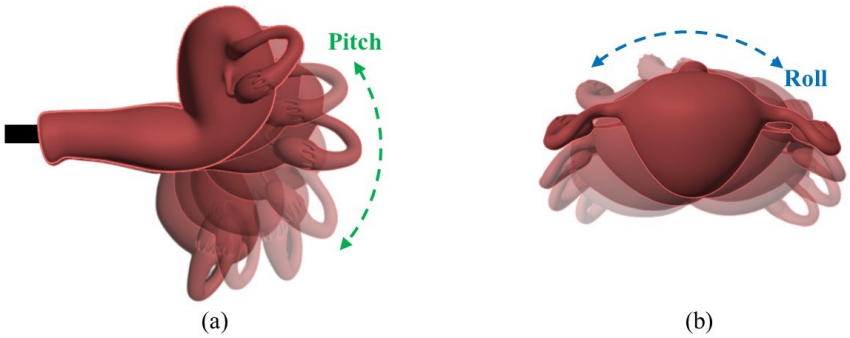

Figure 13. Pitch (**a**) and **Roll** (**b**) motion composite pictures of a 3D uterus model.

According to the test results of the cervical displacement, together with the mathematical model and the 3D uterus model, it was found that the model movement was correct according to the control equation.

3.5. Force Test for Choosing the Actuator

Next, instrument–uterus force was tested to deal with the physical interaction between the proposed uterine manipulator robot and uterus weight as its environment. The goal was to choose an appropriate actuator to guarantee sufficient force could be delivered. The setup for evaluating instrument-uterus force was designed and tested as shown in Figure 14. An AMF-500N Digital Force Gauge Push and Pull Tester was used as the digital force gauge. The force, $\mathbf{F}_{all}$, used to control the instrument was measured with a digital force gauge. Table 3 lists the measured force at different loads and **Pitch** angles ($\boldsymbol{\varphi}$). There were five different clay-lump weights, varying from 100 to 500 g, which covered the average typical uterus weights, representing five uterus weights, where 0 g represents no load, only the bare instrument without any uterus weight.

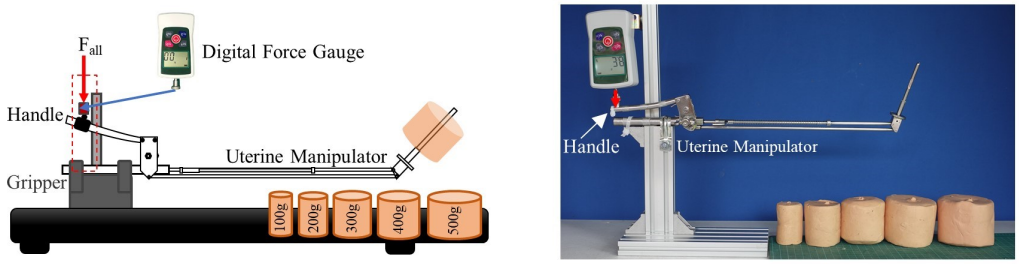

Figure 14. The design (**a**) and experimental setup (**b**) for force assessment.

Table 3. Measured force at different loads and **Pitch** angles (φ).

Pitch Angle (φ)	0 g	100 g	200 g	300 g	400 g	500 g
30°	3.2 N	3.8 N	4.5 N	6.0 N	7.0 N	10.2 N
60°	3.9 N	4.4 N	5.7 N	6.7 N	7.0 N	11.5 N
90°	4.1 N	7.9 N	8.7 N	9.6 N	10.7 N	12.3 N

The next section explains the design and implementation of this proposed model.

3.6. Prototype Design

Last but not least, along with the required force from the assessment above, electric actuators were chosen in preference to other common actuators, such as hydraulic and pneumatic actuators. As a result, the fluid or air from these actuators could leak, and also the electric ones could deliver both precise control and the compact design. To be specific, two stepper motors were chosen to control the **Roll** and **Pitch** motions. As their movement comprises discrete steps with high reliability, low cost, and high torque at low speeds, this makes stepper motors suitable for robotic applications both commercially and industrially when precision positioning is required. In this system, both stepper motors are part of an open loop system for computer-controlled holding and positioning of the uterine manipulator in place, as shown in Figure 15, along with the CAD model and the implemented prototype with all the details. M1 is the stepper motor controlling the $\boldsymbol{\theta}$ in the **Roll** (rotating) panel, where M2 is a mechanical linear actuator with the other motor at the handle controlling the $\boldsymbol{\varphi}$ in the **Pitch** (tilting) panel by converting the distance **d** into the $\boldsymbol{\varphi}$. Per the control interface for the proposed uterine manipulator robot, in order to control the robot in the distance without having to stand at the vaginal end where the uterine manipulator robot takes place, a common two-axes with one-enable-button joystick, adequate for controlling **Roll** and **Pitch** motions step by step, has been deployed in the system. Tilting the lever leftward or rightward controls the M1, increasing or decreasing the **Roll** angle by one degree. Similarly, tilting the lever forward or backward once controls the M2, increasing or decreasing the **Pitch** angle also by one degree. Meanwhile, holding the lever in any direction would change the angle every 0.5 s.

Although the differences for each angle would be a positive value for the counter-clockwise direction and negative value for the clockwise direction, the number of motor steps for M1 and M2 is calculated based on the absolute angle difference values; abs($\boldsymbol{\theta}$) and abs($\boldsymbol{\varphi}$), respectively, as shown in Equations (8) and (9). The constants used in these equations are as follows: **SPR** is the number of steps per revolution; **SPD** is the number of steps per degree = SPR/360°; **L** is the axial distance traveled by the lead screw thread in a single revolution; $\mathbf{d}_{max}$ is the stroke length, the maximum controlling distance at the handle; $\boldsymbol{\varphi}_{max}$ is the maximum pitch angle, which is +90° in this case.

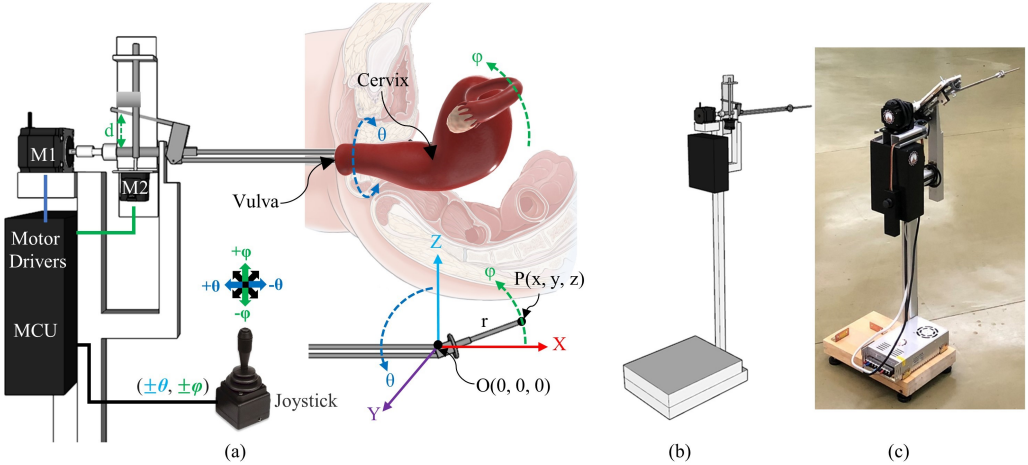

Figure 15. The design (**a**), CAD Model (**b**) and implemented (**c**) of the proposed robotic system.

$$\#of\ M1\ Steps = \mathbf{SPD} \tag{8}$$

$$\#of\ M2\ Steps = \left(\frac{\left(\frac{\mathbf{d}_{max}}{\boldsymbol{\varphi}_{max}}\right) \times \mathbf{SPR}}{\mathbf{L}}\right) \tag{9}$$

After we obtained the maximum force of 12.3, which corresponds to the maximum possible weight (500 g) of a uterus at the **Pitch** angle of 90°, it was determined that this would be the requirement for choosing an appropriate motor that can support this force. The NEMA17, a two-phase hybrid stepping motor, used as a bipolar stepper motor with a 1.8° step angle, has been chosen for the linear actuator, M2, in this study. Each phase draws 1.2 A at 4 V, allowing for a holding torque of 52 N·cm. Though the choice for the stepper motor, M1, is rather straightforward to pick as it does not rely on the uterus weight, only that it has enough force to roll, in any case, the NEMA17 has also been chosen here.

4. Results and Discussion

After designing and implementing the prototype of the uterine manipulator robot according to the essential requirements and criteria as explained in the previous sections, this section presents the results of testing the proposed uterine manipulator robot.

There are ethical limitations in human research with regard to experimenting on real uteruses. Fortunately, as technology advances, there are several alternative ways to conduct experiments on human beings. Theoretically, a soft-tissue cadaver has historically been considered the nearest condition to humans in terms of shape and structure; hence, its use become favored as the best approach for education and research. However, the main disadvantage of using a human cadaver is the cost. Furthermore, facilities must be equipped to properly maintain and store a cadaver, which can be an additional expense. Hence, prior to performing an experiment on a costly soft-tissue cadaver, a 1:1 soft silicone uterus manikin model was built for the early stages of this experiment. The results from experiments on both a uterus manikin model and on five soft-tissue cadavers are presented here.

4.1. Silicone Uterus Manikin Model Test

A 1:1 soft silicone manikin model of a similar size and shape to a real uterus was built to be used in the experiment. Measuring 8 cm in length, 5 cm in width, and 4 cm thick, and with a length of 9.6 cm from vulva to cervix, the uterus manikin model comes with a 300 g weight, the maximum weight most gynecologists would recommend for LAVH. Figure 16 shows the overlap of motion composite images of the silicone uterus manikin model being manipulated by the robot, with (0∼75°) **Pitch** and (±45°) **Roll** motions, while Figure 17 depicts each case when varying **Pitch** angles to 0°, 25°, 50°, and 75°; and **Roll** angles to −45°, 0°, and 45°.

Figure 16. The motion composites of the uterus manikin model; (**a**) side view, and (**b**) front view.

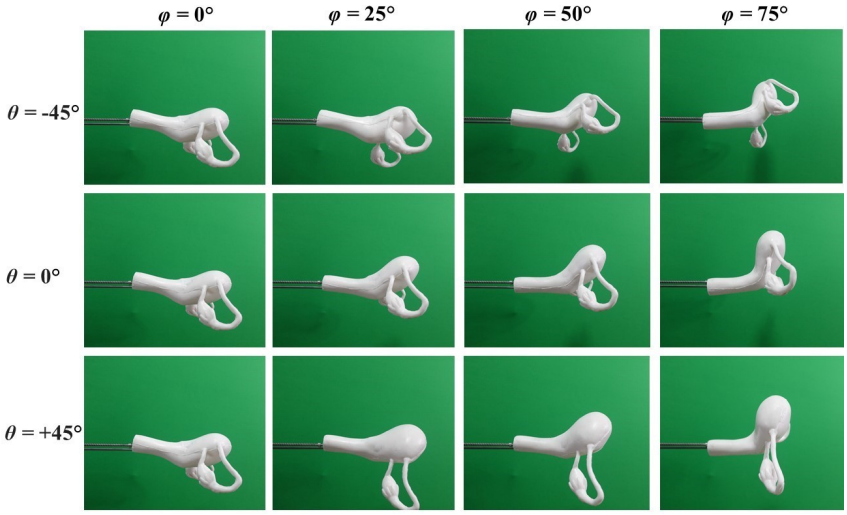

Figure 17. The uterus manikin model with varied **Pitch** and **Roll** angles.

This experiment aimed to confirm that the load capacity of the proposed robot system meets the requirements and to verify the feasibility of the robot's movement in all directions. Moreover, it offers a good way to train the surgeons and assistants to become familiar with how to maneuver the robot. The experimental results show that both DoFs of the proposed robot were successfully achieved, the orientation and coordinate transformations of the instrument tip were altered, and the positions of the uterus manikin model were changed as controlled.

4.2. Soft-Tissue Cadaveric Cases

Subsequently, five soft-tissue cadavers donated for educational research to Srinagarind Hospital, KKU, Thailand, were used in this study, with the Ethical approval #HE641206, waived by the Center for Ethics in Human Research, Khon Kaen University (KKU), on 13 May 2021. The first two cases were used for the requirement gathering process, then later, the proposed robot prototype was applied to a total laparoscopic hysterectomy in three soft-tissue cadavers. Figure 18 illustrates the layout of the operating theater, where the surgical assistant at the vaginal end was replaced by the uterine manipulator robot, which was controlled remotely via a joystick.

Figure 19 shows the laparoscopic views of the experiments conducted on a cadaver with the help of extra light through a medium-size incision in the abdomen. Figure 19a–c,e depict when the **Roll** angle (θ) = 0° with varied **Pitch** angles (φ) (0°, 20°, 40°, and 60°, respectively), while Figure 19d,f depicts when the motion **Pitch** angles (φ) = 60° but the **Roll** angles (θ) are 20° and −20°.

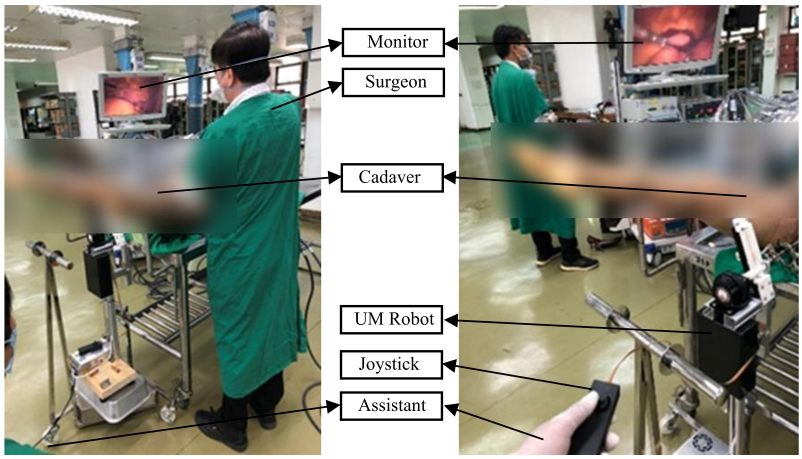

Figure 18. Operating theater layout for soft-tissue cadaveric experiments.

In addition to smoothly manipulating the uterus at the angular velocity of 4 degrees/second (0.67 RPM), the uterine manipulator robot also can steadily manipulate the uterus to various **Roll** and **Pitch** angles, exposing the root of the uterus along with other pelvic organs. According to the experimental surgeries in all five soft-tissue cadavers conducted in this work, the motions in the **Pitch** and **Roll** panels, which are required in a real operation, would involve only 30∼80° and ±15°, respectively. Although these requirements are well within the capabilities of the proposed uterine manipulator robot involving (0∼90°) and ±150° in the **Pitch** and **Roll** panels, respectively, if this robot is implemented as a fixed-tip uterine manipulator with RCM mechanism, as is the case for other previous related robots, those angles could cause discomfort around the vulva area where the instrument is inserted. As a result, the proposed robot incorporating the tiltable-tip uterine manipulator could be more beneficial in this respect.

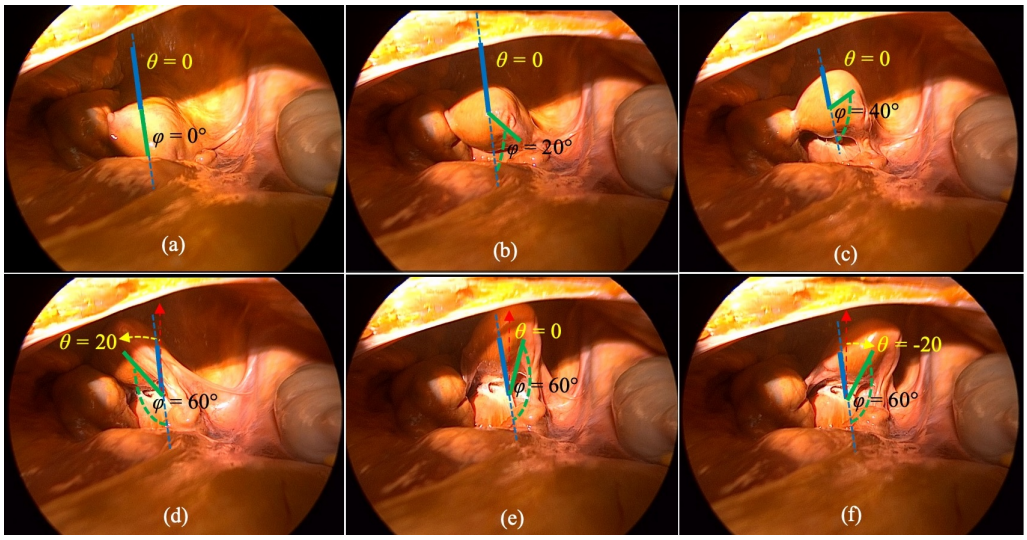

Figure 19. The results with extra external light during cadaver experiments; (**a**–**c**,**e**) showing when the **Roll** angle (***θ***) = 0° with varied **Pitch** angles (***φ***) (0°, 20°, 40°, and 60°, respectively), while (**d**,**f**) showing when the motion **Pitch** angles (***φ***) = 60° but the **Roll** angles (***θ***) are 20° and −20°.

A design of a non-RCM 2-DoF robotic uterine manipulation system has been described for application in laparoscopic gynecologic surgery. The idea is to work with an existing, reusable and tiltable-tip uterine manipulator. A specific instrument has been chosen as a showcase here. However, the common design can be applied to any other tiltable-tip uterine manipulator, while a fixed-tip uterine manipulator would require an RCM mechanism.

To date, this work has been designed and implemented carefully and tested extensively through simulations, models, and experiments on soft-tissue cadavers. Once ethical approval for research on human subjects is granted, this work could proceed to a clinical trial. The setup could remain the same as in experiments on soft-tissue cadavers, with the whole robotic system covered by a sterilized cover to avoid direct contact with the patient, and the uterine manipulator and the joystick will also be sterilized.

5. Conclusions

The use of a uterine manipulator has been commonly credited with the benefit of improving visualization, especially during laparoscopic gynecologic surgery. This paper has presented a new intelligent fatigue-free robotic uterine manipulation system, which has been designed and implemented to cooperate with an existing (1), reusable (2) and tiltable-tip (3) uterine manipulator. These three specific features of the chosen uterine manipulator used in the proposed robotic system offer the surgeon familiarity, cost consciousness, sterilization, and great control range of the instrument without the need for an RCM mechanism which can cause tears or fissures in the vulva. The proposed robot system has been designed to be mounted on a mobile platform, allowing it to be integrated into the existing surgical theater setting. With only two actuators, controlled via a remote joystick along two motion panels, resulting in 2 DoFs with the motion capability of (0∼90°) and (±150°) in the **Pitch** and **Roll** panels, respectively, the proposed system has been found effective and meets the requirement of a uterine manipulator with the ability to support a load of up to 500 g. The paper has also manifested the thorough test results of the proposed design via a mathematical model and a 3D uterus model. Once the prototype was implemented, intensive experiments were conducted and evaluated through a 1:1 uterus manikin model and a total of five soft-tissue cadaver cases. The feedback from all five surgeons, who performed the last three experiments using the proposed prototype on three donated soft-tissue cadavers, was consistent with the purpose of the study, stating that the proposed robotic uterine manipulation system could fulfill the adequate motion angles of (30∼80°) in the **Pitch** panel and (±15°) in the **Roll** panel with the optimal motion control speed at 0.67 RPM. This system could, therefore, serve as an efficient assistant in maneuvering the uterine manipulator, in order to provide the surgeon an ideal view during laparoscopic surgery and improve the efficiency of the surgery. As for future studies, further research concerning reliability and safety of the system (i.e. force detection and feedback control) should be explored before the system can be used in real human trials.

Author Contributions: Conceptualization, K.K.; methodology, S.N. and D.H.; software, S.N. and A.B.; validation, S.N. and D.H.; investigation, S.N. and D.H.; writing—original draft preparation, S.N. and D.H.; writing—review and editing, S.N. and D.H.; supervision, D.H. All authors have read and agreed to the published version of the manuscript.

Funding: Songphon Namkhun was supported by a research grant from the Thai Government Scholarship by NSTDA (National Science and Technology Development Agency).

Institutional Review Board Statement: Ethical review and approval were waived for this study because this study has met the criteria of the Khon Kaen University Ethics Committee for Human Research (KKUEC)'s Exemption Determination Regulations for the Research studying bones, skeletons, extracted teeth, and cadavers.

Informed Consent Statement: Not applicable.

Data Availability Statement: The original contributions presented in the study are included in the article, further inquiries can be directed to the corresponding author.

Acknowledgments: The authors express their gratefulness to the individuals who donated their bodies for anatomical research and study, which could contribute to an improvement of overall knowledge and effective patient care. Therefore, these donors and their families deserve our greatest gratitude.

Conflicts of Interest: The authors declare no conflicts of interest.

References

1. Siddaiah-Subramanya, M.; Tiang, K.W.; Nyandowe, M. A New Era of Minimally Invasive Surgery: Progress and Development of Major Technical Innovations in General Surgery Over the Last Decade. *Surg. J.* **2017**, *3*, e163–e166. [CrossRef]
2. Puntambekar, S.P.; Patil, A.M.; Rayate, N.V.; Puntambekar, S.S.; Sathe, R.M.; Kulkarni, M.A. A Novel Technique of Uterine Manipulation in Laparoscopic Pelvic Oncosurgical Procedures: "The Uterine Hitch Technique". *Minim Invasive Surg.* **2010**, *2010*, 836027. [CrossRef]
3. Mettler, L.; Nikam, Y.A. A Comparative Survey of Various Uterine Manipulators Used in Operative Laparoscopy. *Gynecol. Surg.* **2006**, *3*, 239–243. [CrossRef]
4. ALLY Uterine Positioning System-CooperSurgical. Available online: https://www.coopersurgical.com/product/ally-uterine-positioning-system/ (accessed on 5 March 2024).
5. Side-Kick Basic Holder. Available online: http://www.kronner.com/sidekick.php (accessed on 5 June 2023).
6. The Development of Uterine Manipulator Holder for Gynecologic Laparoscopic Surgery. *Jpn. J. Gynecol. Obstet. Endosc.* **2004**, *20*, 68–69. [CrossRef]
7. Yip, H.M.; Li, P.; Liu, Y. Design and Development of a Robotic Assistant for Uterus Manipulation in Total Laparoscopic Hysterectomy. In Proceedings of the 2014 IEEE International Conference on Information and Automation (ICIA), Hailar, China, 28–30 July 2014; pp. 356–361. [CrossRef]
8. Akrivos, N.; Barton-Smith, P. A Pilot Study of Robotic Uterine and Vaginal Vault Manipulation: The ViKY Uterine Positioner™. *J. Robot. Surg.* **2013**, *7*, 371–375. [CrossRef] [PubMed]
9. Maheshwari, M.; Ind, T. Concurrent Use of a Robotic Uterine Manipulator and a Robotic Laparoscope Holder to Achieve Assistant-Less Solo Laparoscopy: The Double ViKY. *J. Robot. Surg.* **2015**, *9*, 211–213. [CrossRef] [PubMed]
10. Yip, H.M.; Wang, Z.; Navarro-Alarcon, D.; Li, P.; Liu, Y.; Cheung, T.H. A New Robotic Uterine Positioner for Laparoscopic Hysterectomy with Passive Safety Mechanisms: Design and Experiments. In Proceedings of the 2015 IEEE/RSJ International Conference on Intelligent Robots and Systems (IROS), Hamburg, Germany, 28 September–2 October 2015; pp. 3188–3194. [CrossRef]
11. Yip, H.M.; Wang, Z.; Navarro-Alarcon, D.; Li, P.; Cheung, T.H.; Greiffenhagen, C.; Liu, Y.-H. A Collaborative Robotic Uterine Positioning System for Laparoscopic Hysterectomy: Design and Experiments. *Int. J. Med. Robot.* **2020**, *16*, e2103. [CrossRef] [PubMed]
12. Premachra, H.A.G.C.; Herath, H.M.A.N.; Thathsarana, K.M.; Liyanage, D.L.F.M.; Amarasinghe, Y.W.R.; Madusanka, D.G.K.; Jayawardane, M.A.M.M. Design and Development of a Robotic Uterine Manipulator for Gynecological Laparoscopy. In Proceedings of the 2022 8th International Conference on Control, Automation and Robotics (ICCAR), Xiamen, China, 8–10 April 2022; pp. 145–154. [CrossRef]
13. Wu, J.; Chen, W.; Guo, D.; Ma, G.; Wang, Z.; He, Y.; Zhong, F.; Lu, B.; Wang, Y.; Cheung, T.H.; et al. Robot-Enabled Uterus Manipulator for Laparoscopic Hysterectomy with Soft RCM Constraints: Design, Control, and Evaluation. *IEEE Trans. Med. Robot. Bionics* **2022**, *4*, 656–666. [CrossRef]
14. Wu, J.; Wang, T.; Guo, H.; Wang, Y.; Guo, D.; Lu, B.; Wang, Z.; Zhong, F.; Wang, H.; Yuan, J.; et al. Design, Control, and Experiments of a Novel Robotic Uterine Manipulator with the Motorized 3-DoF Manipulation Rod. *IEEE Trans. Biomed. Eng.* **2023**, *70*, 2203–2214. [CrossRef] [PubMed]
15. Tsai, W.-N. A Novel Uterine Manipulator Incorporating Non-Local Controls and Lateral Motion. Bachelor's Thesis, Massachusetts Institute of Technology, Cambridge, MA, USA, 2013. Available online: https://dspace.mit.edu/handle/1721.1/83748 (accessed on 15 March 2023).
16. Nguyen, V.S.; Hwang, B.; Lee, S.; Kim, S.; Kim, B. Three Degrees of Freedom-Based Master–Slave Uterine Manipulation Robot System for Laparoscopic Hysterectomy. *J. Mech. Robot.* **2022**, *15*, 021001. [CrossRef]
17. Barnhart, K.T.; Izquierdo, A.; Pretorius, E.S.; Shera, D.M.; Shabbout, M.; Shaunik, A. Baseline Dimensions of the Human Vagina. *Hum. Reprod.* **2006**, *21*, 1618–1622. [CrossRef] [PubMed]
18. Sengul, M.; Selim, H.S. Comparison of Uterine Manipulators Types in Total Laparoscopic Hysterectomy: A Retrospective Study. *Pak. J. Med. Sci.* **2023**, *39*, 961–966. [CrossRef] [PubMed]
19. Husslein, H.; Frecker, H.; Shore, H.; Lefebvre, E.M.; Latta, G.; Montanari, E.; Satkunaratnam, A. Comparing two Uterine Manipulators During Total Laparoscopic Hysterectomy: A Randomized Controlled Trial. *J. Minim. Invasive Gynecol.* **2017**, *24*, 764–771. [CrossRef] [PubMed]
20. TINTARA Uterine Manipulator | KARL STORZ Endoskope | . Available online: https://www.karlstorz.com/th/en/product-detail-page.htm?productID=1000144388&cat=1000194507 (accessed on 2 March 2024).
21. Mustaza, S. Modelling and Control of a Flexible Soft Robotic Uterine Elevator. Ph.D. Thesis, Department of Electrical and Electronic Engineering, Faculty of Engineering and Physical Sciences, Surrey University, Guildford, UK, 2018. [CrossRef]
22. Lee, S.; Kang, H.; Hwang, B.; Kim, B. Design and Evaluation of a Bending Actuator for a Robotic Uterine Manipulator, based on a McKibben Pneumatic Artificial Muscle. *J. Korean Soc. Manuf. Technol. Eng.* **2020**, *29*, 413–421. [CrossRef]
23. Abdel Khalek, Y.; Bitar, R.; Christoforou, C.; Garzon, S.; Tropea, A.; Biondi, A.; Sleiman, Z. Uterine Manipulator in Total Laparoscopic Hysterectomy: Safety and Usefulness. *Updat. Surg.* **2020**, *72*, 1247–1254. [CrossRef]
24. Wang, Z.; Zhang, W.; Ding, X. A Family of RCM Mechanisms: Type Synthesis and Kinematics Analysis. *Int. J. Mech. Sci.* **2022**, *231*, 107590. [CrossRef]

25. Shi, H.; Liang, Z.; Zhang, B.; Wang, H. Design and Performance Verification of a Novel RCM Mechanism for a Minimally Invasive Surgical Robot. *Sensors* **2023**, *23*, 2361. [CrossRef] [PubMed]
26. DeLancey, J.O.L. The Anatomy of the Pelvic Floor. *Curr. Opin. Obstet. Gynecol.* **1994**, *6*, 313. [CrossRef] [PubMed]
27. Yavuzcan, A.; Altıntaş, R.; Yıldız, G.; Başbuğ, A.; Baştan, M.; Çağlar, M. Does Uterine Manipulator Type Affect Surgical Outcomes of Laparoscopic Hysterectomy? *Gynecol. Minim Invasive Ther.* **2021**, *10*, 19–24. [CrossRef] [PubMed]
28. van den Haak, L.; Alleblas, C.; Rhemrev, J.P.; Scheltes, J.; Nieboer, T.E.; Jansen, F.W. Human Cadavers to Evaluate Prototypes of Minimally Invasive Surgical Instruments: A Feasibility Study. *Technol. Health Care* **2017**, *25*, 1139–1146. [CrossRef] [PubMed]
29. Matplotlib Python. Available online: https://matplotlib.org/ (accessed on 1 January 2023).
30. Blender Foundation. Available online: https://www.blender.org/ (accessed on 10 March 2023).